Chapter 3

Measuring Process Capability Based on C_{PK} with Gauge Measurement Errors

C_{PK} was created in Japan to offset some of the weaknesses in C_P, primarily the fact that C_P measured capability in terms of process variation only and did not take process location into consideration. From observing the definition of C_{PK} ($C_{PK} = \min\{C_{PU}, C_{PL}\}$, see equation (1.3)), it is apparent that C_{PK} quantifies capability for the worst half of the data, i.e. C_{PK} is quantified only by the worst-tail to specification limit relationship, thus, the individual effects of process location and variation on process capability are confounded in this index.

Under the normal assumption, process yield is given by

$$\%\text{yield} = 100\left[\Phi\left(\frac{USL-\mu}{\sigma}\right)-\Phi\left(\frac{LSL-\mu}{\sigma}\right)\right]. \tag{3.1}$$

Boyles [2] gave the upper and lower bounds on %yield associated with C_{PK} as

$$100\left[2\Phi(3C_{PK})-1\right] \le \%\text{yield} \le 100\left[\Phi(3C_{PK})\right]. \tag{3.2}$$

And, Finley [9] developed a table of approximate proportion NC associated with given C_{PK} values (see Table 6).

Table 6. Approximate proportion NC associated with given C_{PK} values.

C_{PK}	Parts outside tolerance limits
0.25	16 out of 100
0.5	7 out of 100
1.0	13 out of 10 000
1.33	3 out of 100 000
1.67	1 out of 1000 000
2.0	1 out of 1000 000 000

In section 3.1, we discuss the ratio r between the empirical process capability C_{PK}^{Y} and the true process capability C_{PK}. In section 3.2, we obtain the pdf, the expected value, the variance and the MSE of $\hat{C}_{PK}^{Y}$. And, we compare the MSE of $\hat{C}_{PK}^{Y}$ with that of $\hat{C}_{PK}$. In section 3.3, we use the confidence interval bounds in Pearn & Shu [39] to estimate the minimum process capability by $\hat{C}_{PK}^{Y}$, we show that a large measurement error results in significantly underestimating the true process capability. In section 3.4, we use the critical values in Pearn & Lin

[37] to test whether the process capability meets the requirement, and we show that the α-risk and the power both become decrease with measurement error. In section 3.5, we present our modified confidence interval bounds and critical values for the cases that measurement errors are unavoidable. Finally in section 3.6, an example is presented.

3.1 Empirical Process Capability C_{PK}^{Y}

Suppose that X ~ Normal (μ , σ^2) represents the relevant quality characteristic of a manufacturing process, and C_{PK} measures the true process capability. However in practice, the observed variable Y is measured rather than the true variable X. Assume that X and M are stochastically independent, we have Y ~ Normal (μ, $\sigma_Y^2 = \sigma^2 + \sigma_M^2$), and the empirical process capability index C_{PK}^{Y} is obtained after substituting σ_Y for σ. The relationship between the true process capability C_{PK} and the empirical process capability C_{PK}^{Y} can be expressed as

$$\frac{C_{PK}^{Y}}{C_{PK}} = \frac{1}{\sqrt{1+\lambda^2 C_P^2}}. \tag{3.3}$$

Since the variation of data we observed is larger than the variation of the original data, the denominator of the index C_{PK} becomes larger, and the true capability of the process is understated if calculation of process capability index is based on empirical data Y.

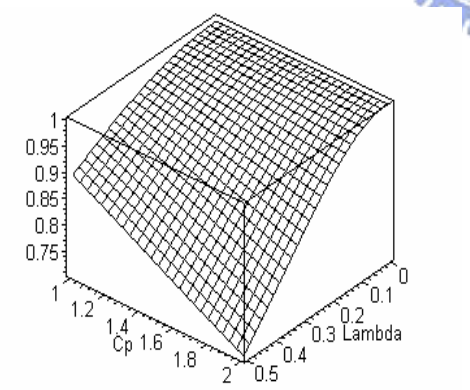

Figure 7(a). Surface plot of r with $C_P \in [1, 2]$ for $\lambda \in [0, 0.5]$.

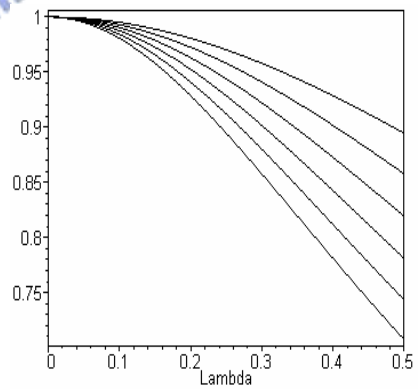

Figure 7(b). Plots of r versus $\lambda \in [0, 0.5]$ for $C_P = 1.0(0.2)2.0$.

Figure 7(a) displays the surface plot of the ratio $r = C_{PK}^{Y} / C_{PK}$ for $\lambda \in [0, 0.5]$ with $C_P \in [1, 2]$. Figure 7(b) plots the ratio r versus λ for $C_P = 1.0(0.2)2.0$. Those figures show that the measurement errors result in a decrease in the estimate. Small process variation has the same effect as the presence of measurement error does. Since r would be small if λ becomes large, the gauge becomes more important as the true capability improves. For instance, If $\lambda = 0.5$ and $C_P = 2$ (the ratio $r = 0.71$), $C_{PK}^{Y} = 0.36$ with $C_{PK} = 0.50$, and

C_{PK}^{Y} = 1.78 with C_{PK} = 2.50. The empirical process capability diverges from the true process capability more with large measurement errors.

3.2 Sampling Distribution of $\hat{C}_{PK}^{Y}$

In practice, sample data must be collected in order to estimate the empirical process capability. Suppose that the empirical data (observed measurement contaminated with errors) $\{ Y_i,\ i = 1, 2, ..., n \}$ is collected, then the natural estimator $\hat{C}_{PK}^{Y}$ defined as the following,

$$\hat{C}_{PK}^{Y} = \frac{d - |\bar{Y} - m|}{3S_Y}, \tag{3.4}$$

which is obtained by replacing the process mean μ and the process standard deviation σ by their conventional estimators $\bar{Y} = \sum_{i=1}^{n} Y_i / n$ and $S_Y = [\sum_{i=1}^{n} (Y_i - \bar{Y}) / (n-1)]^{1/2}$, from a demonstrably stable process.

Applying the same technique used in Pearn & Lin [37], and Kotz & Johnson [18], we obtain the cdf of $\hat{C}_{PK}^{Y}$ as

$$F_{\hat{C}_{PK}^{Y}}(x) = 1 - \int_0^{3C_P^Y\sqrt{n}} G\left(\frac{(n-1)(3C_P^Y\sqrt{n} - t)^2}{9nx^2} \right) f_T^Y(t)dt\ , \tag{3.5}$$

where $f_T^Y(t) = \Phi[t + 3(C_P^Y - C_{PK}^Y)\sqrt{n}] + \Phi[t - 3(C_P^Y - C_{PK}^Y)\sqrt{n}]$, $C_P^Y = C_P / \sqrt{1 + \lambda^2 C_P^2}$, and $C_{PK}^{Y} = C_{PK} / \sqrt{1 + \lambda^2 C_P^2}$. The mean and the variance of the estimator $\hat{C}_{PK}^{Y}$ are

$$\mathrm{E}(\hat{C}_{PK}^{Y}) = \frac{1}{3b_{n-1}} \left\{ b^Y - \sqrt{\frac{2}{n\pi}} \exp(-\frac{n}{2}(\xi^Y)^2) - |\xi^Y| \left[1 - 2\Phi(-\sqrt{n}\,|\xi^Y|) \right] \right\}, \tag{3.6}$$

$$\mathrm{Var}(\hat{C}_{PK}^{Y}) = \frac{n-1}{9(n-3)} \left\{ (b^Y)^2 - 2b^Y \left[\sqrt{\frac{2}{n\pi}} \exp(-\frac{n}{2}(\xi^Y)^2) + |\xi^Y| (1 - 2\Phi(-\sqrt{n}\,|\xi^Y|)) \right] \right.$$

$$\left. + (\xi^Y)^2 + \frac{1}{n} \right\} - (E(\hat{C}_{PK}^{Y}))^2, \tag{3.7}$$

where $b^Y = 3C_P^Y$ and $\xi^Y = 3(C_P^Y - C_{PK}^Y)$. The mean and the variance of $\hat{C}_{PK}^{Y}$ are very lengthy, and cannot be further simplified. To investigate how measurement errors may affect the sample distribution, we conduct some bias and the MSE analysis. Noting that from the expression $C_{PK} = C_P - |\xi|/3$ (or $C_P = C_{PK} + |\xi|/3$), Pearn & Lin [37] and Pearn & Shu [39] showed that the lower confidence bounds and critical values for C_{PK} can be obtained by setting $\xi = 1.00$. Therefore, here we set $C_P = C_{PK} + 1/3$ and consider cases of (C_P, C_{PK}) = (1.33, 1.00) and (1.83, 1.50) for illustrations.

Figures 8(a)-8(b) plot the bias of $\hat{C}_{PK}^{Y}$ versus n = 5(1)100 with λ = 0(0.1)0.5 for (C_P, C_{PK}) = (1.33, 1.00) and (1.83, 1.50). Figures 9(a)-9(b) are the

surface plots of the ratio $\gamma_2 = \text{MSE}(\hat{C}_{PK}^{Y}) / \text{MSE}(\hat{C}_{PK})$ with $n = 5(1)100$ and $\lambda \in$ in [0, 0.5] for $(C_P, C_{PK}) = (1.33, 1.00)$ and (1.83, 1.50). It is noted that when $\lambda = 0$, the bias of $\hat{C}_{PK}^{Y}$ equals to the bias of $\hat{C}_{PK}$, but the bias of $\hat{C}_{PK}^{Y}$ decreases as λ increases. In some cases, $\hat{C}_{PK}^{Y}$ may be unbiased while $\hat{C}_{PK}$ will never be, but the absolute bias of $\hat{C}_{PK}^{Y}$ may be much greater than that of $\hat{C}_{PK}$ for large λ. It is observed from Figures 9(a)-9(b) that γ_2 varies in n or λ, particularly for large C_{PK}. For large n, the value γ_2 is greater than 1 ($\text{MSE}(\hat{C}_{PK}^{Y}) > \text{MSE}(\hat{C}_{PK})$) for most λ, and γ_2 increases in λ. The maximum values of γ_2 in Figures 9(a)-9(b) are 10.055 and 15.785 respectively, and the minimum values of γ_2 in Figures 9(a)-9(b) are 0.756 (1/1.323) and 0.584 (1/1.712) respectively. All the maximum values of γ_2 occur at $(n, \lambda) = (100, 0.5)$, and all the minimum values of γ_2 occur at $(n, \lambda) = (5, 0.5)$. The difference between $\text{MSE}(\hat{C}_{PK}^{Y})$ and $\text{MSE}(\hat{C}_{PK})$ with $\gamma_2 > 1$ is more significant than that with $\gamma_2 < 1$.

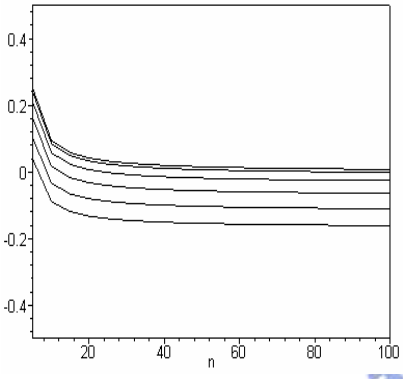

Figure 8(a). Plots of the bias of $\hat{C}_{PK}^{Y}$ for $n = 5(1)100$, $\lambda = 0(0.1)0.5$ (top to bottom), $C_P = 1.33$ and $C_{PK} = 1.00$.

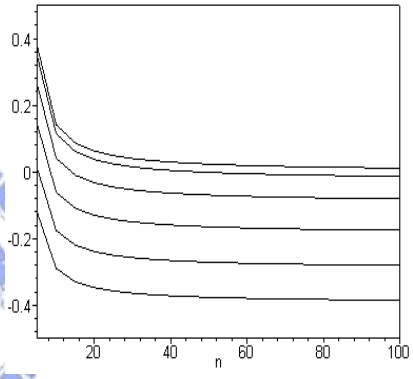

Figure 8(b). Plots of the bias of $\hat{C}_{PK}^{Y}$ for $n = 5(1)100$, $\lambda = 0(0.1)0.5$ (top to bottom), $C_P = 1.83$ and $C_{PK} = 1.50$.

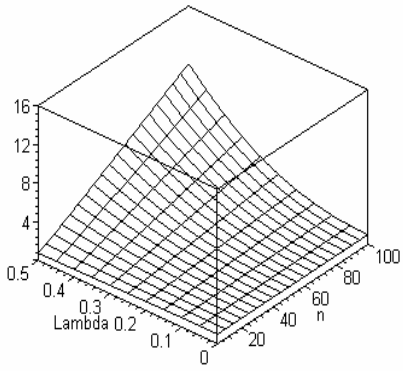

Figure 9(a). Surface plot of γ_2 with $n = 5(1)100$ and $\lambda \in [0, 0.5]$ for $C_P = 1.33$ and $C_{PK} = 1.00$.

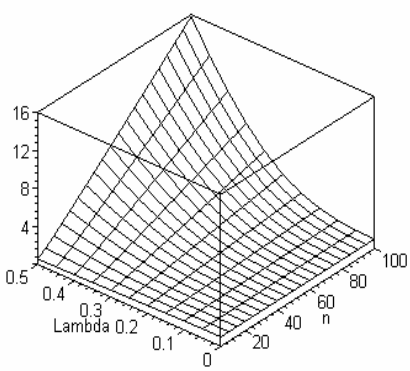

Figure 9(b). Surface plot of γ_2 with $n = 5(1)100$ and $\lambda \in [0, 0.5]$ for $C_P = 1.83$ and $C_{PK} = 1.50$.

3.3 Lower Confidence Bound Based on $\hat{C}_{PK}^{Y}$

The lower confidence bounds estimate the minimum process capability based on sample data. To find reliable $100\theta\%$ lower confidence bound L_K for

C_{PK} (θ represents the probability that the confidence interval contains the actual C_{PK}), Pearn & Shu [39] solved the following equation,

$$\int_0^{b\sqrt{n}} G\left(\frac{(n-1)(b\sqrt{n}-t)^2}{9n(\hat{C}_{PK})^2}\right)\left[\Phi(t+\xi\sqrt{n})+\Phi(t-\xi\sqrt{n})\right]dt = 1-\theta. \tag{3.8}$$

Noting that $b = 3C_P$ can be expressed as $b = 3L_K + |\xi|$. Since the process parameters μ and σ are unknown, then the distribution characteristic parameter $\xi = (\mu - m)/\sigma$ is also unknown. To eliminate the need for further estimating the distribution characteristic parameter ξ, Pearn & Shu [39] examined the behavior of the lower confidence bound L_K against the parameter ξ. They performed extensive calculations to obtain the lower confidence bound values L_K for $\xi = 0(0.05)3.00$, $\hat{C}_{PK} = 0.7(0.1)3.0$, $n = 10(5)200$ with confidence coefficient $\theta = 0.95$. They found that the lower confidence bound L_K obtains its minimum at $\xi = 1.00$ in all cases. Thus for practical purpose they recommended to solve equation (3.8) with $\xi = \hat{\xi} = 1.00$ to obtain the required lower confidence bounds, without having to further estimate the parameter ξ.

But, $\hat{C}_{PK}^Y$ is substituted into equation (3.8) to obtain the confidence bounds, which can be written as (we denote the bound originated from $\hat{C}_{PK}^Y$ as L_K^Y),

$$\int_0^{(3L_K^Y+1)\sqrt{n}} G\left(\frac{(n-1)[(3L_K^Y+1)\sqrt{n}-t]^2}{9n(\hat{C}_{PK}^Y)^2}\right)\left[\Phi(t+\sqrt{n})+\Phi(t-\sqrt{n})\right]dt = 1-\theta. \tag{3.9}$$

The confidence coefficient by the confidence bound L_K^Y (denoted by θ^Y) is

$$\theta^Y = 1-\int_0^{(3L_K^Y+\xi^Y)\sqrt{n}} G\left(\frac{(n-1)[(3L_K^Y+\xi^Y)\sqrt{n}-t]^2}{9n(\hat{C}_{PK}^Y)^2}\right)\left[\Phi(t+\hat{\xi}^Y\sqrt{n})+\Phi(t-\hat{\xi}^Y\sqrt{n})\right]dt, \tag{3.10}$$

where $\xi^Y = 3(C_P - C_{PK})$, and $\hat{\xi}^Y = 3(\hat{C}_P^Y - \hat{C}_{PK}^Y)$. Since $\hat{C}_{PK}^Y$ is smaller than $\hat{C}_{PK}$, and L_K^Y is smaller than L_K, then θ^Y is always greater than θ. Figures 10(a)-10(b) plot L_K^Y versus $\lambda \in [0, 0.5]$ with $n = 50$, $\hat{C}_{PK} = 1.00$, 1.50, and $\hat{C}_P = \hat{C}_{PK} + \gamma_3$, $\gamma_3 = 0.33$, 0.50, 0.67, and 1.00 for 95% confidence intervals (for sufficiently large sample size n, we have $\hat{C}_{PK}^Y = \hat{C}_{PK} / \sqrt{1+\lambda^2\hat{C}_P^2}$. Therefore, we set $\hat{C}_{PK}^Y = \hat{C}_{PK} / \sqrt{1+\lambda^2\hat{C}_P^2}$ to obtain $\hat{C}_{PK}^Y$ in Figures 10(a)-10(b)). We see that in Figures 10(a)-10(b), L_K^Y decreases in λ, especially for large $\hat{C}_P$ values, and the decrement of L_K^Y is more significant for large $\hat{C}_{PK}$. A large measurement error results in significantly underestimating the true process capability.

In current practice, a process is called "inadequate" if $C_{PK} < 1.00$, "marginally capable" if $1.00 \le C_{PK} < 1.33$, "satisfactory" if $1.33 \le C_{PK} < 1.50$, "excellent" if $1.50 \le C_{PK} < 2.00$, and "super" if $2.00 \le C_{PK}$. If capability

measures do not include the measurement errors, significant underestimation of the true process capability may result in high production cost, losing the power of competition. For instance, suppose that a process has a 95% lower confidence bound, 1.236 ($\hat{C}_{PK} = 1.50$) with $n = 50$, which meets the threshold of an "excellent" process. But the bound may be calculated as 0.983 with measurement errors $\lambda = 0.30$ and the process is determined as "inadequate".

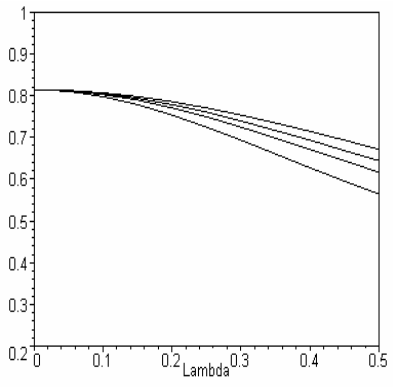

Figure 10(a). Plots of L_K^Y versus λ with $n = 50$ for $\hat{C}_P = 1.33, 1.50, 1.67, 2.00$ (top to bottom) and $\hat{C}_{PK} = 1.00$.

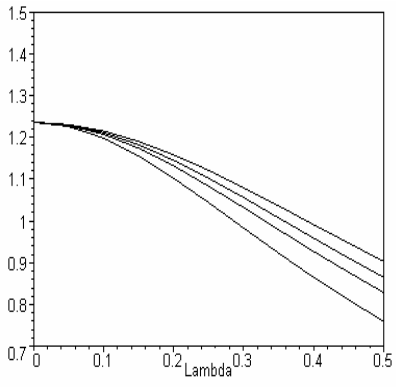

Figure 10(b). Plots of L_K^Y versus λ with $n = 50$ for $\hat{C}_P = 1.83, 2.00, 2.17, 2.50$ (top to bottom) and $\hat{C}_{PK} = 1.50$.

3.4 Capability Testing Based on $\hat{C}_{PK}^Y$

To determine if a given process meets the preset capability requirement, we could consider the statistical testing with null hypothesis $H_0: C_{PK} \leq c$ (process is not capable) and alternative hypothesis $H_0: C_{PK} > c$ (process is capable), where c is the required process capability. If the calculated process capability is greater than the corresponding critical value, we reject the null hypothesis and conclude that the process is capable. Suppose that the nominal size of the statistical testing is α, the critical value c_0 can be determined by solving the following equation,

$$\int_0^{3C_P\sqrt{n}} G\left(\frac{(n-1)(3C_P\sqrt{n}-t)^2}{9nc_o^2}\right)\left[\Phi[t+3(C_P-c)\sqrt{n}]+\Phi[t-3(C_P-c)\sqrt{n}]\right]dt = \alpha \tag{3.11}$$

with test power

$$\pi(C_{PK}) = P\left(\hat{C}_{PK} \geq c_0 \mid C_{PK}, C_P\right)$$

$$= \int_0^{3C_P\sqrt{n}} G\left(\frac{(n-1)(3C_P\sqrt{n}-t)^2}{9nc_o^2}\right)\left[\Phi[t+3(C_P-C_{PK})\sqrt{n}]+\Phi[t-3(C_P-C_{PK})\sqrt{n}]\right]dt\,. \tag{3.12}$$

To eliminate the need for estimating the characteristic parameter C_P, Pearn & Lin [37] examined the behavior of the critical values c_0 against the parameter C_P. They performed extensive calculations to obtain the critical values c_0 for $C_P = c(0.01)(c+1)$, $c = 1.00, 1.33, 1.50, 1.67$, and 2.00, $n = 10$ (50) 300, and $\alpha = 0.05$. They found that the critical values c_0 obtains its maximum at $C_P = c + 1/3$ in all cases. For practice purpose, they recommended to solve equation (3.11) with $C_P = c + 1/3$ to obtain the required critical values, without having to further estimate the parameter C_P.

Thus, the α-risk corresponding to the test using the sample estimate $\hat{C}_{PK}^{Y}$ (denoted by α^Y) will become

$$\alpha^Y = P\left(\hat{C}_{PK}^{Y} \geq c_0 \,|\, C_{PK} = c, C_P = c + 1/3\right)$$

$$= \int_0^{3C_P^Y\sqrt{n}} G\left(\frac{(n-1)(3C_P^Y\sqrt{n}-t)^2}{9nc_o^2}\right)\left[\Phi[t+3(C_P^Y - C_{PK}^Y)\sqrt{n}] + \Phi[t-3(C_P^Y - C_{PK}^Y)\sqrt{n}]\right]dt\,, \tag{3.13}$$

where $C_P^Y = (c+1/3)/\sqrt{1+\lambda^2(c+1/3)^2}$, and $C_{PK}^Y = c/\sqrt{1+\lambda^2(c+1/3)^2}$. The test power (denoted by π^Y) is

$$\pi^Y = P\left(\hat{C}_{PK}^{Y} \geq c_0 \,|\, C_{PK}, C_P = c + 1/3\right)$$

$$= \int_0^{3C_P^Y\sqrt{n}} G\left(\frac{(n-1)(3C_P^Y\sqrt{n}-t)^2}{9nc_o^2}\right)\left[\Phi[t+3(C_P^Y - C_{PK}^Y)\sqrt{n}] + \Phi[t-3(C_P^Y - C_{PK}^Y)\sqrt{n}]\right]dt\,, \tag{3.14}$$

where $C_P^Y = (C_{PK}+1/3)/\sqrt{1+\lambda^2(C_{PK}+1/3)^2}$, and $C_{PK}^Y = C_{PK}/\sqrt{1+\lambda^2(C_{PK}+1/3)^2}$.

Earlier discussions indicate that the true process capability would be severely underestimated if $\hat{C}_{PK}^{Y}$ is used. The probability that $\hat{C}_{PK}^{Y}$ is greater than c_0 would be less than that of using $\hat{C}_{PK}$. Thus, the α-risk using $\hat{C}_{PK}^{Y}$ is less than the α-risk if using $\hat{C}_{PK}$ when estimating C_{PK}. The test power if using $\hat{C}_{PK}$ is also less than the test power of using $\hat{C}_{PK}$. That is, $\alpha^Y \leq \alpha$ and $\pi^Y \leq \pi$. Figures 11(a)-11(b) are the surface plots of α^Y with $n = 5(1)100$, $\lambda \in [0, 0.5]$ for $c = 1.00, 1.50$, and $\alpha = 0.05$. Figures 12(a)-12(b) plot π^Y versus λ with $n = 50$, $\alpha = 0.05$, for $c = 1.00, 1.50$, and $C_{PK} = c(0.20)(c+1)$. Note that for $\lambda = 0$, $\alpha^Y = \alpha$ and $\pi^Y = \pi$. In Figures 11(a)-11(b), α^Y decreases as λ or n increases, and the decreasing rate is more significant with large c. In fact, for large λ, α^Y is smaller than 1×10^{-5}. In Figures 12(a)-12(b), π^Y decreases as λ increases, but increases as n increases. Decrement of π^Y in λ is more significant for large c. In the presence of measurement errors, π^Y may decrease substantially. For instance, in Figure 12(b), the π^Y value ($c = 1.50$, $n = 50$) for $C_{PK} = 2.30$ is $\pi^Y =$

0.994 if there is no measurement error ($\lambda = 0$). But, when $\lambda = 0.5$, π^Y decreases to 0.012, the decrement of the power is 0.982.

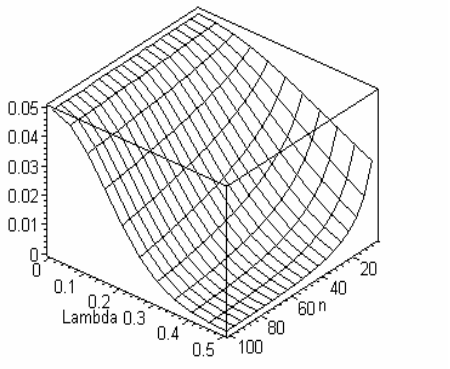

Figure 11(a). Surface plot of α^Y with $n = 5(1)100$ and $\lambda \in [0, 0.5]$ for $c = 1.00$ and $\alpha = 0.05$.

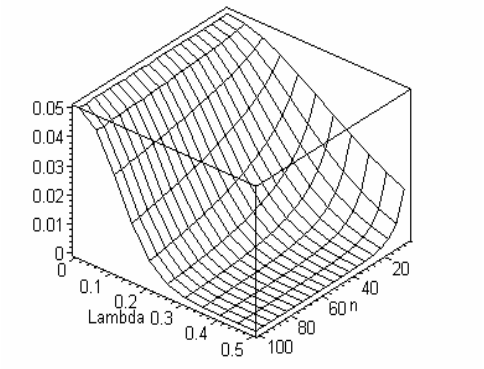

Figure 11(b). Surface plot of α^Y with $n = 5(1)100$ and $\lambda \in [0, 0.5]$ for $c = 1.50$ and $\alpha = 0.05$.

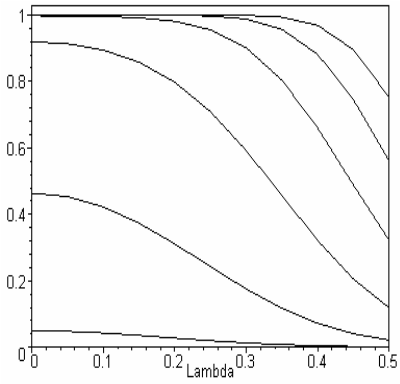

Figure 12(a). Plots of π^Y versus λ with $n = 50$, $\alpha = 0.05$ for $c = 1.00$, $C_{PK} = 1.00(0.20)2.00$ (bottom to top).

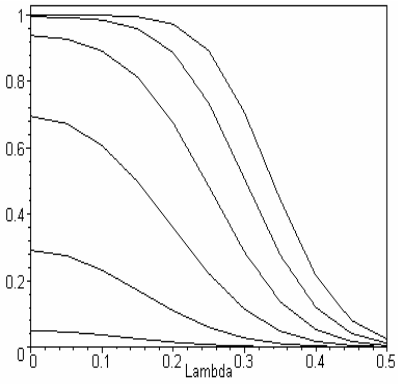

Figure 12(b). Plots of π^Y versus λ with $n = 50$, $\alpha = 0.05$ for $c = 1.50$, $C_{PK} = 1.50(0.20)2.50$ (bottom to top).

3.5 Modified Confidence Bounds and Critical Values

We showed earlier that the coefficients increase due to underestimating the lower confidence bounds. We also showed that the α-risk and the test power decrease with measurement error. The probability of passing non-conforming product units decreases, but the probability of correctly judging a capable process as incapable also decreases. Since the lower confidence bound is severely underestimated and the power becomes small, the producers cannot firmly state that their processes meet the capability requirement even if their processes are sufficiently capable. Good product units would be incorrectly rejected in this case. Unnecessary cost may accompany those incorrect decisions to the producers. Improving the gauge capability and training the operators by proper education are essential to measurement error reduction. Nevertheless, measurement errors are unavoidable in most industry applications. In this section, we consider the adjustment of confidence bounds and critical values to

provide better capability assessment.

Suppose that the desired confidence coefficient is θ, the adjusted confidence interval of C_{PK} with lower confidence bound L_K^*, can be established as

$$\theta = P\left(C_{PK} > L_K^*\right)$$

$$= 1 - \int_0^{b^*\sqrt{n}} G\left(\frac{(n-1)(b^*\sqrt{n}-t)^2}{9n(\hat{C}_{PK}^Y)^2}\right)\left[\Phi(t+\hat{\xi}^Y\sqrt{n}) + \Phi(t-\hat{\xi}^Y\sqrt{n})\right] dt\,, \qquad (3.15)$$

where $b^* = 3L_K^*/\sqrt{1+\lambda^2 C_P^2} + |\xi^Y|$. To eliminate the need for estimating the characteristic parameter ξ^Y, we follow the method of Pearn and Shu [39] by setting $\xi^Y = 1.00$ to find the adjusted lower confidence bound L_K^*, where C_P can be obtained by equation $3(C_P - L_K^*)/\sqrt{1+\lambda^2 C_P^2} = 1.00$, as

$$C_P = \frac{18L_K^* + \sqrt{324{L_K^*}^2 - 4(9-\lambda^2)(9{L_K^*}^2 - 1)}}{2(9-\lambda^2)} = C_{P1} \qquad (3.16)$$

Figures 13(a)-13(b) are comparisons among L_K, L_K^Y, and L_K^* for $\hat{C}_{PK} = 1.00, 1.50$ with $n = 50$, where L_K is the 95% lower confidence bound using $\hat{C}_{PK}$, L_K^Y is the 95% lower confidence bound using $\hat{C}_{PK}^Y$, and L_K^* is the adjusted 95% lower confidence bound using $\hat{C}_{PK}^Y$ ($\hat{C}_{PK}^Y = \hat{C}_{PK}/\sqrt{1+\lambda^2\hat{C}_P^2}$ is also used to obtain $\hat{C}_{PK}^Y$). In this case, the probability that the lower confidence interval with bound L_K^Y contains the actual C_{PK} value is greater than that of the interval with the bound L_K or L_K^*, while the probability that the lower confidence interval with bound L_K or L_K^* contains the actual C_{PK} value is 0.95. From Figures 13(a)-13(b), we see that the lower confidence bounds remained underestimated, even if it is adjusted. But, the magnitude of underestimation using the adjusted confidence bound is significantly reduced.

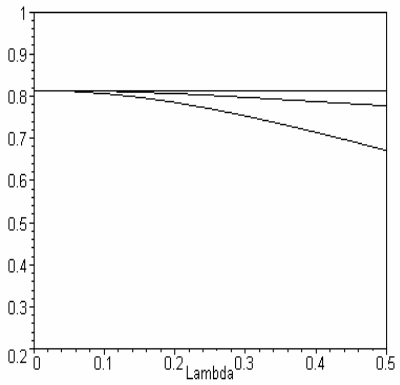

Figure 13(a). Plots of L_K, L_K^*, and L_K^Y (top to bottom) versus λ with $n = 50$ and for $\hat{C}_{PK} = 1.00$.

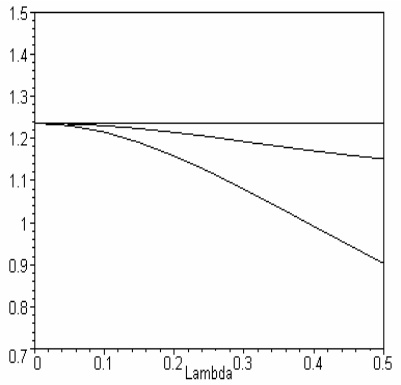

Figure 13(b). Plots of L_K, L_K^*, and L_K^Y (top to bottom) versus λ with $n = 50$ and for $\hat{C}_{PK} = 1.50$.

In order to improve the test power, we revise the critical values c_0^* to satisfy $c_0^* < c_0$. Thus, the probability $P\{\hat{C}_{PK}^Y > c_0^*\}$ is greater than $P\{\hat{C}_{PK}^Y > c_0\}$. Both the α-risk and the test power increase when we use c_0^* as a new critical value in the testing. Suppose that the α-risk using the revised critical value c_0^* is α^*, the revised critical values c_0^* can be determined by

$$\alpha^* = P\left(\hat{C}_{PK}^Y \geq c_0^* \mid C_{PK} = c\right)$$

$$= \int_0^{3C_P^Y\sqrt{n}} G\left(\frac{(n-1)(3C_P^Y\sqrt{n}-t)^2}{9n(c_o^*)^2}\right)\Phi[t+3(C_P^Y - C_{PK}^Y)\sqrt{n}] + \Phi[t-3(C_P^Y - C_{PK}^Y)\sqrt{n}]dt\,, \tag{3.17}$$

where $C_P^Y = C_P/\sqrt{1+\lambda^2 C_P^2}$, and $C_{PK}^Y = c/\sqrt{1+\lambda^2 C_P^2}$. To eliminate the need for further estimating the characteristic parameter C_P, we follow the method described in Pearn and Lin [37] by setting $C_P^Y = C_{PK}^Y + 1/3$ to find the adjusted critical values c_0^*, where C_P can be obtained by the equation $C_P/\sqrt{1+\lambda^2 C_P^2} = c/\sqrt{1+\lambda^2 C_P^2} + 1/3$, as

$$C_P = \frac{18c + \sqrt{324c^2 - 4(9-\lambda^2)(9c^2-1)}}{2(9-\lambda^2)} = C_{P2}\,. \tag{3.18}$$

To ensure that the α-risk is within the preset magnitude, we let $\alpha^* = \alpha$ and solve the equation to obtain c_0^*. The power (denoted by π^*) can be calculated as

$$\pi^*(C_{PK}) = P\left(\hat{C}_{PK}^Y \geq c_0 \mid C_{PK}, C_P = C_{P2}\right)$$

$$= \int_0^{3C_P^Y\sqrt{n}} G\left(\frac{(n-1)(3C_P^Y\sqrt{n}-t)^2}{9n(c_o^*)^2}\right)\left[\Phi(t+\sqrt{n}) + \Phi(t-\sqrt{n})\right]dt\,, \tag{3.19}$$

where $C_P^Y = C_{PK}^Y + 1/3$, and $C_{PK}^Y = C_{PK}/\sqrt{1+\lambda^2 C_{P2}^2}$.

Figures 14(a)-14(b) are plots of π^* versus λ with $n = 50$, $\alpha = 0.05$, for $c = 1.00$, 1.50 and $C_{PK} = c(0.20)(c+1)$. From those figures, we see that the powers corresponding to the adjusted critical values c_0^* remain decreasing in measurement error, but the decrements are much smaller. We improve the test power to a certain degree. For instance, when we compare the π^Y values in Figure 12(b) ($c = 1.50$, $n = 50$) to the π^* values in Figure 14(b) ($c = 1.50$, $n = 50$), we obtain that $\pi^Y = 0.012$ and $\pi^* = 0.992$ with $\lambda = 0.5$. In this case, using the adjusted critical values c_0^*, we improve the test power by 0.980 (which is rather significant). For our results to be practical, we tabulate the revised critical values for some commonly used capability requirements in Tables 16-19 in the Appendix. Using those tables, the practitioner may omit the complex calculation and simply select the proper critical values for capability testing.

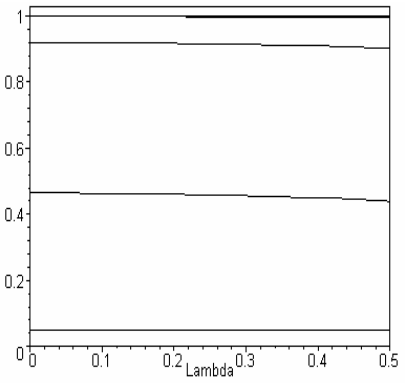

Figure 14(a). Plots of π^* versus λ with $n = 50$, $\alpha = 0.05$ for $c = 1.00$, $C_{PK} = 1.00(0.20)2.00$ (bottom to top).

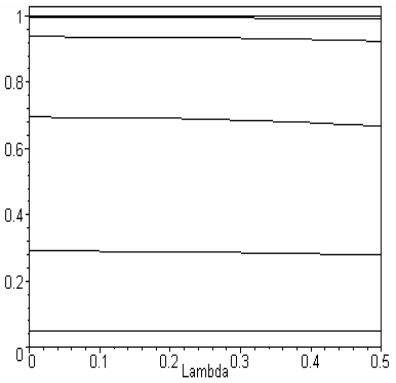

Figure 14(b). Plots of π^* versus λ with $n = 50$, $\alpha = 0.05$ for $c = 1.50$, $C_{PK} = 1.50(0.20)2.50$ (bottom to top).

3.6 Application Example

The *LM* 2576 series of regulators, as depicted in Figures 15(a)-15(b), are monolithic integrated circuits, which provide the active functions for a step-down (buck) switching regulator, capable of driving 3A load with excellent line and load regulation. Those devices are available in fixed output voltages of 3.3V, 5V, 12V, 15V, and an adjustable output version. Requiring a minimum number of external components, those regulators are simple to use and include internal frequency compensation and a fixed-frequency oscillator. The *LM* 2576 series offers a high-efficiency replacement for popular three-terminal linear regulators. It substantially reduces the size of the heat sink, and in some cases no heat sink is required. A standard series of inductors optimized for use with the *LM* 2576 are available from several different manufacturers. This feature greatly simplifies the design of switch-mode power supplies. Other features include a guaranteed $\pm 4\%$ tolerance on output voltage within specified input voltages and output load conditions, and $\pm 10\%$ on the oscillator frequency. External shutdown is included, featuring 50 μA (typical) standby current. The output switch includes cycle-by-cycle current limiting, as well as thermal shutdown for full protection under fault conditions.

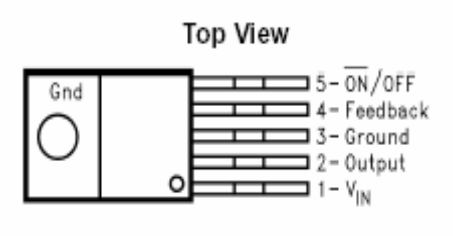

Figure 15(a). *LM*2576 series step-down voltage regulator product (top view).

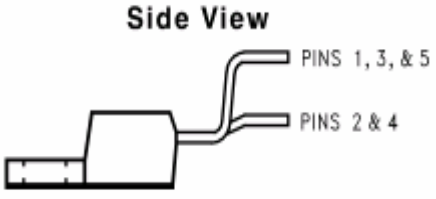

Figure 15(b). *LM*2576 series step-down voltage regulator product (side view).

Table 7. 70 observations for output voltage (unit: V)

3.292	3.289	3.293	3.323	3.279	3.304	3.306	3.288	3.287	3.319
3.299	3.269	3.300	3.294	3.308	3.285	3.292	3.278	3.285	3.282
3.297	3.278	3.311	3.295	3.319	3.303	3.305	3.326	3.315	3.298
3.321	3.315	3.284	3.319	3.302	3.314	3.308	3.303	3.294	3.312
3.297	3.305	3.306	3.295	3.286	3.293	3.288	3.314	3.318	3.295
3.309	3.296	3.296	3.305	3.293	3.298	3.305	3.289	3.288	3.315
3.308	3.279	3.292	3.293	3.265	3.283	3.307	3.314	3.303	3.305

Consider a supplier manufacturing step-down voltage regulator products in Taiwan, making *LM* 2576-3.3 type with specifications of output voltage: T = 3.3V, USL = 3.366V, LSL = 3.234V for conditions of V_{IN} = 12V (input voltage), I_{LOAD} = 0.5A (load current), and T_J = 25 ^{0}C (temperature). A total of 70 observations are collected and displayed in Table 7. Histogram and normal probability plot show that the collected data follows the normal distribution. Shapiro-Wilk test is applied to further justify the assumption. To determine whether the process is "excellent" (C_{PK} > 1.50) with unavoidable measurement errors λ = 0.25, we first determine that c = 1.50 and α = 0.05. Then, based on the sample data of 70 observations, we obtain the sample mean $\bar{Y}$ = 3.299, the sample standard deviation S_Y = 0.013, and the point estimator $\hat{C}_{PK}^{Y}$ = 1.632. From Table A7, we obtain the critical value c_0^* = 1.595 based on α, λ and n. Since $\hat{C}_{PK}^{Y}$ > c_0^*, we therefore conclude that the process is "excellent". Moreover, by inputting $\hat{C}_{PK}^{Y}$, λ, n, and the desired confidence coefficient θ = 0.95 into the computer program we obtain the 95% lower confidence bound of the true process capability as 1.542. We can see that if we ignore the measurement errors and evaluate the critical value without any correction, the critical value may be calculated as c_0 = 1.758. In this case would reject that the process is "excellent" since $\hat{C}_{PK}^{Y}$ is no greater than the uncorrected critical value 1.758.